Key Points:
- High-resolution large-ensemble simulations are used to assess changes in global tropical cyclone activity under +4 K surface warming
- Future changes in tropical cyclone activity are investigated in a more objective manner
- Total number of very intense tropical cyclones decreases contrary to some previous studies, but occurrences increase in several regions

Correspondence to:
K. Yoshida,
kyoshida@mri-jma.go.jp

Future Changes in Tropical Cyclone Activity in High-Resolution Large-Ensemble Simulations

Kohei Yoshida[1], Masato Sugi[1], Ryo Mizuta[1] (iD), Hiroyuki Murakami[1,2], and Masayoshi Ishii[1] (iD)

[1]Meteorological Research Institute, Tsukuba, Japan, [2]Geophysical Fluid Dynamics Laboratory, Princeton, NJ, USA

Abstract Projected future changes in global tropical cyclone (TC) activity are assessed using 5,000 year scale ensemble simulations for both current and 4 K surface warming climates with a 60 km global atmospheric model. The global number of TCs decreases by 33% in the future projection. Although geographical TC occurrences decrease generally, they increase in the central and eastern parts of the extra tropical North Pacific. Meanwhile, very intense (category 4 and 5) TC occurrences increase over a broader area including the south of Japan and south of Madagascar. The global number of category 4 and 5 TCs significantly decreases, contrary to the increase seen in several previous studies. Lifetime maximum surface wind speeds and precipitation rate are amplified globally. Regional TC activity changes have large uncertainty corresponding to sea surface temperature warming patterns. TC-resolving large-ensemble simulations provide useful information, especially for policy making related to future climate change.

1. Introduction

The influence of future global warming on tropical cyclone (TC) activity attracts considerable attention from both scientific and socioeconomic viewpoints because of the potential consequences of TCs for fatalities and societal disruption. Possible future changes in TC activity (such as the genesis frequency, occurrence frequency, maximum wind speeds, minimum sea level pressure, and mean precipitation) have been investigated using observational records and global and regional model simulations (see Lighthill et al., 1994; McBride et al., 2006). Recent studies have fostered a consensus that high-resolution global models are useful for assessing possible future changes in TC activity. Models with different spatial resolution also tend to produce different future changes in TC activity (Bengtsson et al., 2007; Manganello et al., 2014; Murakami et al., 2012; Roberts et al., 2015; Strachan et al., 2013), and thus, high-resolution models finer than 100 km may be most appropriate for assessing the future changes. Recent studies have also shown that the projected future changes in TC activity for each ocean basin have large uncertainty that mainly originates from the patterns of sea surface temperature (SST) warming (e.g., Knutson et al., 2010; Murakami et al., 2012; Sugi et al., 2009). Uncertainty in SST warming strongly affects future changes in large-scale atmospheric circulation such as the Walker circulation (Ma & Xie, 2013).While coupled atmosphere-ocean models participating in phase 5 of the Coupled Model Intercomparison Project (CMIP5) (Taylor et al., 2012) have a wide range of SST warming patterns, the TC structure projected by these models tends to be unrealistic due to shortcomings in model performance, resulting from, for example, their coarse resolution (Camargo, 2013).

A 60 km atmospheric general circulation model of the Meteorological Research Institute of Japan (MRI-AGCM3.2H, hereafter) realistically simulates TC activity mainly because of its high spatial resolution (Murakami et al., 2012). Uncertainties associated with model resolution, model physics, model biases, SST warming patterns, and atmosphere-ocean coupling have been assessed with MRI-AGCM3.2H and related models (Murakami et al., 2012, 2012, 2014; Ogata et al., 2015; Sugi et al., 2016). However, because TCs have both low occurrence frequency and large internal variability, large-ensemble simulations are needed to investigate the detailed probabilistic distribution of TC activity in an uncertain future environment. Therefore, high-resolution, large-ensemble global atmospheric model simulations that adequately cover future SST uncertainty are desired to better assess future TC activity. Thanks to recent improvements in computational power, we have performed 5,000 year scale ensemble simulations with MRI-AGCM3.2H. This simulation data set, the database for Policy Decision making for Future climate change (d4PDF), is available online (at http://www.miroc-gcm.jp/~pub/d4PDF/index_en.html).The d4PDF data set is described briefly in the next section, and details may be found in Kawase et al. (2016) and Mizuta et al. (2016). The present study aims to investigate possible future changes and uncertainty in TC activity with the d4PDF, focusing on internal variability, detailed probabilistic distributions, and extreme events. Section 2 briefly describes the data set

and methods used in this study. Section 3 displays results focusing on probabilistic distributions of TC activity, and section 4 presents an assessment of future changes in major TC activity metrics. Finally, section 5 provides concluding remarks.

2. Experimental Design, Data, and Methods

2.1. Experimental Design

We use the large-ensemble simulation data set for current and future climates, d4PDF, which is produced by MRI-AGCM3.2H (Mizuta et al., 2012). The horizontal resolution is T_L319 (equivalent to a 60 km horizontal grid), there are 64 vertical layers, and the model top is set at 0.01 hPa. The current climate simulations were integrated for 60 years from 1951 to 2010 with observed SSTs and sea ice concentration from COBE-SST2 (Hirahara et al., 2014) and observed global warming gas concentrations. The current climate simulations were constituted by 100 ensemble members based on initial value perturbations of the atmosphere and short-term monthly SST perturbations. The future climate simulations were performed for 60 years with a constant warming condition roughly corresponding to the level of year 2090 in the Representative Concentration Pathway 8.5 (RCP8.5) scenario adopted in CMIP5. Because of the large variety in future SST projections, we chose six SST warming patterns projected by six coupled models: CCSM4, GFDL-CM3, HadGEM2-AO, MIROC5, MPI-ESM-MR, and MRI-CGCM3 (see Figure S1 in supporting information). Each SST warming pattern of the RCP8.5 scenario was scaled by a multiplier, so that MRI-AGCM3.2H reproduces 4 K surface air warming from the preindustrial level. Here the future monthly SSTs were constructed from adding the SST warming patterns to detrended monthly COBE-SST2 from 1951 to 2010. The future climate simulations were constituted by 90 ensemble members based on six future SST patterns and the perturbations mentioned above. See Text S1 in the supporting information and Mizuta et al. (2016) for more details of the experimental design. In the present study, the last 32 years of each of the current and future climate simulations were analyzed, comparing with high quality observational data of tropical cyclones.

2.2. Observational Data

The observational TC track data used in the present study are from the Unisys Weather Hurricane/Tropical data website (Unisys, 2015). This data set is composed of best track TC data provided by the National Hurricane Center and Joint Typhoon Warning Center including location, maximum surface wind speed, and minimum sea level pressure. The best track data for 1979–2010 were used because of the data reliability.

2.3. Tropical Cyclone Tracking Method and Statistical Bias Correction

The TC tracking method and threshold values adopted in this study are the same as those of Murakami et al. (2012). Appropriate thresholds of sea level pressure, 850 hPa relative vorticity, 850 hPa and surface wind speed, warm core temperature, and duration period for the TC tracking are chosen for the model characteristics and resolution (Murakami et al., 2012; Wehner et al., 2015). Consequently, the global number of TC geneses detected in the current climate simulations by MRI-AGCM3.2H is close to that observed. Although other TC tracking methods might affect the interpretation of results, a comparison of two explicit detection methods did not show large differences aside from trivial detection errors (Murakami et al., 2015). Another study reported that discrepancies between TC tracking methods mainly arose from the value of thresholds of TC duration, wind speed, and formation latitude (Horn et al., 2014). The classification of ocean basins for TC assessment follows Murakami et al. (2012): North Indian Ocean (NIO), Western North Pacific (WNP; west of 180°E), Eastern North Pacific (ENP; east of 180°E), North Atlantic (NAT), South Indian Ocean (SIO; west of 135°E), and South Pacific (SPA; east of 135°E).

To adequately assess very intense tropical cyclones, the statistical bias correction used in Sugi et al. (2016) was applied to the simulated maximum surface wind speed. This method modifies the wind speed so that the cumulative distribution function is close to that observed in each 5° latitudinal band and in each ocean basin. Atmosphere-only general circulation models often fail to simulate TC intensity, especially during the decay process in the extratropics. Atmosphere-ocean coupled processes such as oceanic Ekman pumping in shallow oceanic mixed layer are important for TCs (Ogata et al., 2015).The statistical bias correction also reduces these errors in TC intensity.
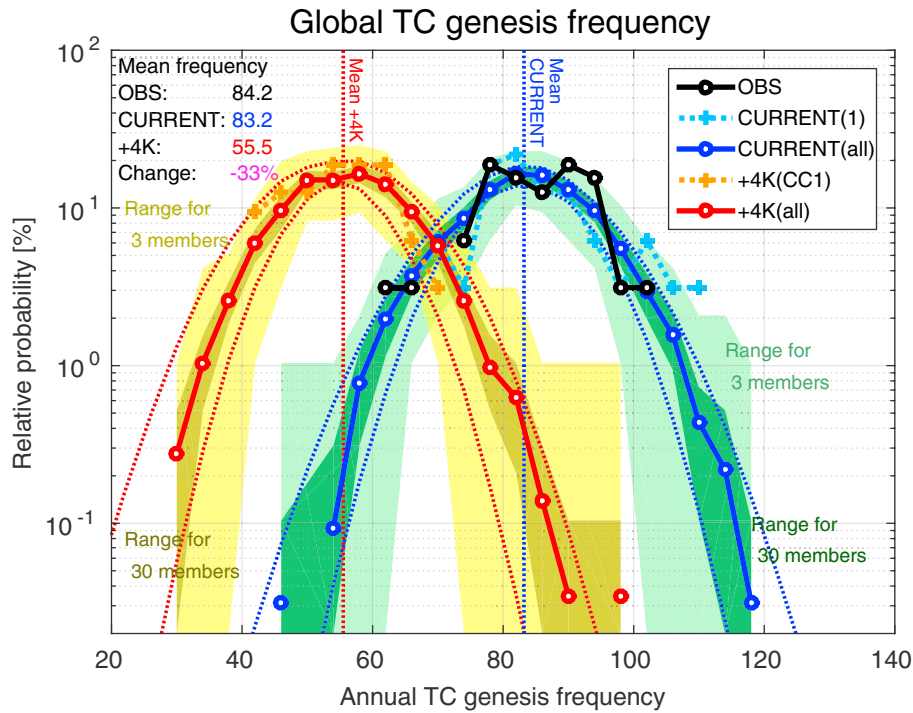
Figure 1. Relative probability distribution of annual tropical cyclone (TC) genesis frequency [counts/year] over the global ocean. Black line is for observations, light blue and blue lines are for a single-member and 100-member of the current climate simulations, respectively, and orange and red lines area single-member (with CCSM4 warming pattern) and 90-member of the future climate simulations, respectively. Shading shows 95% confidence intervals of uncertainty ranges for 3 (light green or light yellow) and 30 (dark green or dark yellow) members of the current and future simulations, respectively. Dotted curves show 95% confidence intervals of normal distributions estimated by three member of the current and future simulations. Each confidence interval is calculated from 1000 sets of ensembles chosen by the bootstrap method. Vertical dotted lines show climatological mean values of TC genesis frequency for the current (blue) and future (red) simulations.

3. Results

3.1. TC Genesis Frequency

Figure 1 shows relative probabilities of annual TC genesis frequency from observations and current and future climate simulations over the global ocean (see Figure S2 for each ocean basin). Even a single-member simulation can represent both the observed climatological mean and interannual variability as well as the all-member results. However, the frequency distribution of the single-member simulation is not smooth due to the small sample size, similar to the observations, whereas the all-member simulations have a smooth frequency distribution, similar to a normal distribution. Mean TC genesis frequency in the future climate decreases by 33% from the climatological mean value of current simulations (83.2 counts/year). Uncertainty ranges of probability distributions for a three-member case, corresponding to a typical ensemble size, and for a 30-member case are also shown as intermediates between the single-member and all-member cases. These uncertainty ranges indicate that as the number of ensemble members increases, the ranges apparently shrink. Additionally, the uncertainty ranges of normal distributions estimated by the three-member set are larger than the uncertainty ranges of directly estimated distributions for the 30-member case and are not adequate for assessing the probability in detail. Unlike the results in the global ocean, the actual probability distributions in individual ocean basins tend to be out of range of estimated normal distributions, especially the NIO, ENP, and NAT (Figure S2). It should be emphasized that these directly estimated probability distributions are the outcomes of explicit global model simulations, not a statistical estimation. Thus, even extremely low probability events—that were not observed so far in a short term but could be observed if sufficient sample of observations is available—may be simulated.

3.2. Geographical Distribution of TC Occurrence

Geographical distributions of TC occurrence frequency, so-called TC days, for all tropical cyclones and for those in category 4 and 5 of the Saffir-Simpson Hurricane wind scale (maximum surface wind speed greater than 59 m/s; CAT45, hereafter) are shown in Figure 2. The current climate simulations reproduce the spatial
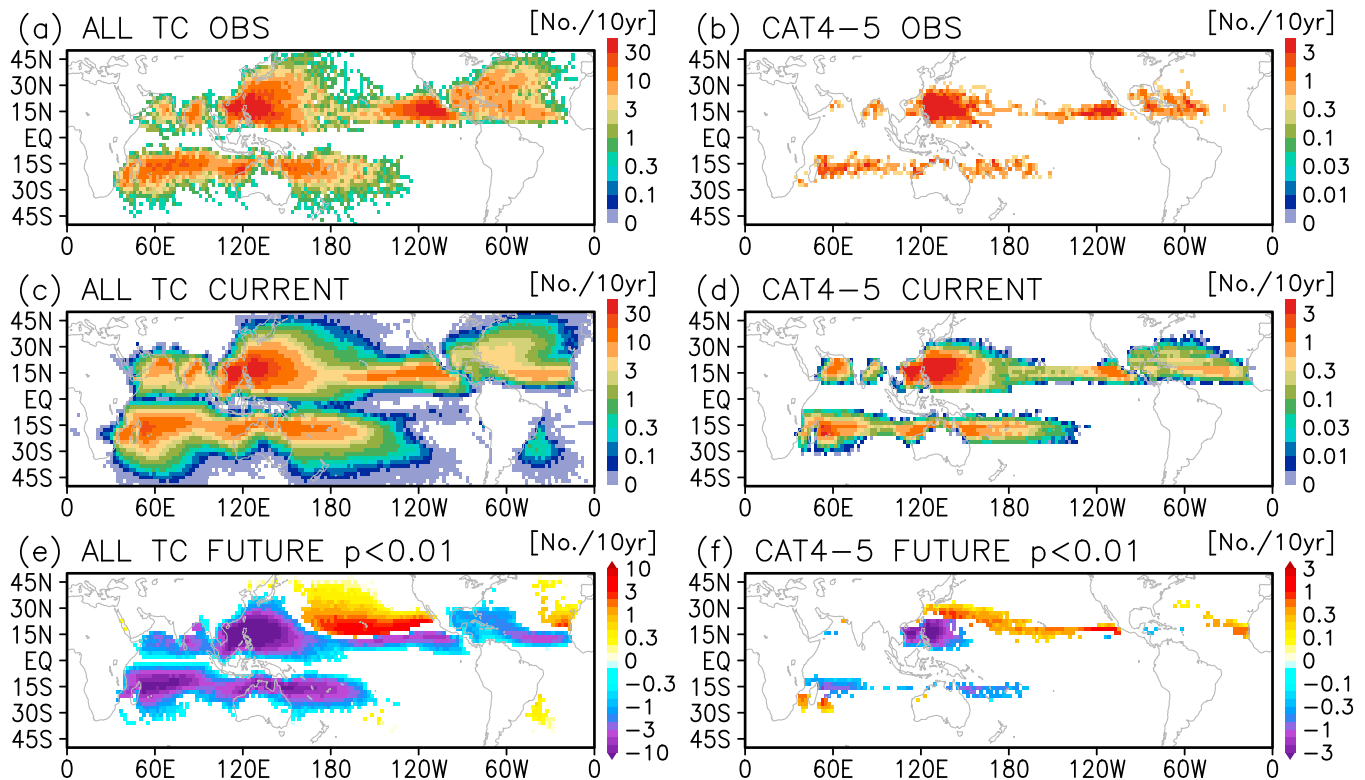
Figure 2. (a, c, and e) TC occurrence frequency (TC days) and (b, d, and f) TC occurrence frequency for CAT45. The observations (Figures 2a and 2b), current climate simulations (Figures 2c and 2d), and future changes (Figures 2e and 2f) shown only for regions that are statistically significant at a 99% confidence level ($p < 0.01$) by the two-sided Mann-Whitney-Wilcoxon test. Unit is the number of occurrences per 10 years in each 2.25° grid cell.

distribution of observed TC occurrence frequency, although the occurrence frequencies of both the all TCs and CAT45 TCs are slightly underestimated in the ENP, NAT, and extratropics of WNP (Figures 2a–2d).The distribution for all ensemble members shows finer and smoother structure than in the observations, resolving regions with frequency smaller than 0.1/10 years (Figure 2c). The TC occurrence distribution for CAT45 presents a realistic and smooth pattern thanks to the bias correction and large sample size (Figure 2d).

Future changes in all TC occurrence frequencies are shown in Figure 2e. The changes are displayed only for areas with statistical significance at a 99% confidence level. The large-ensemble simulations provide a clearer picture of future changes than previous studies (e.g., Knutson et al., 2015).There are significant decreases in TC occurrence in WNP, northwestern parts of SIO, and SPA, and along 10°N of NIO, ENP, and NAT, but significant increases near Hawaii and west of Senegal (Figure 2e). The patterns are basically consistent with previous studies (Knutson et al., 2015; Murakami et al., 2012; Roberts et al., 2015), but the amplitudes of the future changes and the spatial extent of positive change in the North Pacific are slightly different, because of differences in greenhouse gas emission scenarios (SRES-A1B, RCP4.5, or RCP8.5) for future projection, SST warming patterns, and atmospheric models. The increase in TC occurrence around Hawaii is led by a northwestward shift of the main TC development region related to changes in the Walker circulation (Murakami et al., 2013).

Significant decreases in future CAT45 TC occurrence frequency appear in the equatorial parts of WNP, SIO, SPA, and NIO (Figure 2f). Meanwhile, increases are found in an elongated region extending from the west coast of Mexico to the south of Japan and the areas from Bermuda to the west of Senegal and in the south of Madagascar. South of Japan, west of Mexico, and south of Madagascar, future CAT45 TC occurrences increase remarkably despite the overall decrease in TC occurrences there. Future changes in atmospheric circulations such as vertical shear of horizontal wind and vertical wind tend to correspond to CAT45 TC occurrence changes consistent with previous studies (Figure S3). This is the first study presenting statistically robust and spatially detailed future changes in very intense TCs that are of great societal concern. Future changes of geographical CAT45 TC occurrences are shown by Knutson et al. (2015) and Sugi et al. (2016),
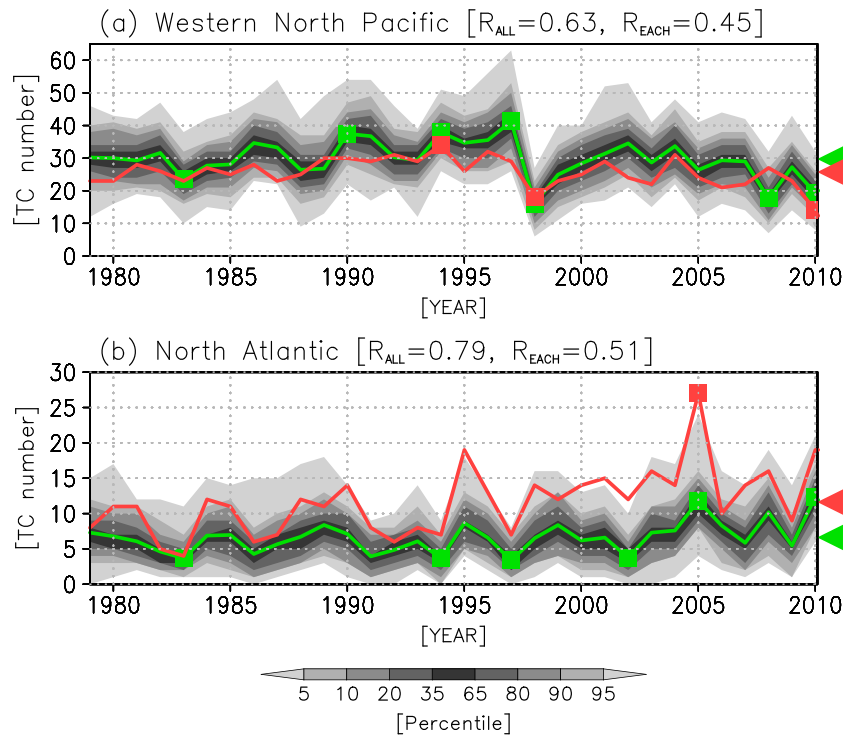
Figure 3. Time series of the number of TC geneses in (a) the western North Pacific and (b) North Atlantic. Red and green lines show observed values and 100 member ensemble mean values of the current climate simulations, respectively. Gray shading depicts percentile values for the 100 member current climate simulations. Squares show that (red) the values are statistically significant at a 90% confidence level (green); the 10th (90th) percentile values are larger (smaller) than climatological means of corresponding time series (triangle). R_{ALL} is the correlation coefficient between observations and the all ensemble mean of the current climate simulations, and R_{EACH} is the average correlation coefficient between observations and individual ensemble members.

with coarse spatial patterns and less statistical significance. However, their results are roughly similar to those of the present study. CAT45 TC occurrence frequency increases in areas from the south of Japan to the tropical central Pacific. By contrast, both the amplitude and area of the changes are different between the studies, especially in the tropical WNP, and the changes are of the opposite sign in the tropics of western SIO and eastern ENP.

3.3. Interannual Variations

Here we discuss the interannual variation in TC genesis frequency in the current climate simulations to assess its reproducibility and the effect of large-ensemble simulations. Figure 3 shows time series of the TC genesis frequency in WNP and NAT. These regions are chosen because of the high correlation between model results and observations. The observed TC genesis frequencies for 1979–2010 mostly fall in the range of the ensemble members of the current climate simulations. The correlation coefficients between the observations and the ensemble means of the current climate simulations are larger than the ensemble mean of correlation coefficients for each member, because the effect of atmospheric internal variations is reduced. The correlation coefficients for WNP (0.63) and NAT (0.78) are much higher than those in the other ocean basins, as shown in previous studies (e.g., Roberts et al., 2015). The observed TC genesis frequency is significantly anomalous in 1994, 1998, and 2010 over WNP, and in 2005 and 2010 over NAT. More than 90% of ensemble members indicate the same sign of anomalies as the observations. Therefore, these anomalous years are likely to be responses to SST variation and to be realized in high probability.

4. Future Change Assessment of TC Activity Metrics

In this section, we assess future changes in four major metrics of TC activity: annual TC genesis frequency, the number of TCs reaching CAT45, lifetime maximum intensity (LMI) of surface wind speed, and mean precipitation rate within 200 km from the TC center when the surface wind speed reaches LMI (Figure 4). The results clearly have high statistical confidence for almost all metrics because of the large-ensemble size.
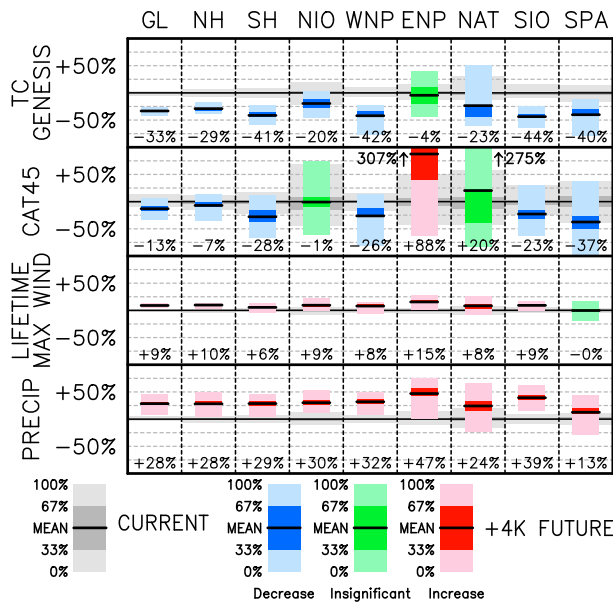
Figure 4. Future changes in the ratios of the TC metrics to the climatological mean in the current climate simulations for the global ocean, the two hemispheres and individual ocean basins. From top to bottom: TC genesis frequency, the number of TCs for CAT45 (≥ 59 m/s maximum surface wind speed), lifetime maximum intensity (LMI) of surface wind, and LMI of precipitation rate averaged within 200 km of the TC center. Black horizontal line displays ensemble mean value. Shading denotes uncertainty ranges for the current climate simulations and future climate simulations.

Globally, the d4PDF suggests a 33% decrease in future TC genesis frequency (see also Figure 1), 13% decrease in the number of CAT45 TCs, 9% increase in LMI of surface wind speed, and 28% increase in LMI of mean precipitation rate. The rate of reduction of the number of CAT45 TCs is smaller than that of TC genesis frequency. Although the overall number of TCs falls, the intensification of the maximum surface wind speed increases the ratio of CAT45 TCs to all TCs by 30%. The reduction (33%) in TC genesis frequency in the present study is larger than that in the Intergovernmental Panel on Climate Change (IPCC) 5th Assessment Report (AR5), partly because the results of IPCC AR5 related to TCs were based on the SRES-A1B scenario (Christensen et al., 2013). According to Murakami et al. (2012), MRI-AGCM3.2H simulates the future reduction of TC genesis frequency at around 24% under the SRES-A1B scenario, which is consistent with the results of IPCC AR5. Additionally, an atmosphere-ocean coupled model, SINTEX-G, simulated a reduction in global TC genesis frequency of about 44% under a quadrupling of atmospheric CO_2 concentration with respect to the preindustrial climate, which corresponds to tropical SST warming of about 3.7 K (Gualdi et al., 2008).

It should be emphasized that the number of CAT45 TCs decreases in the present study, which is the opposite of the changes in IPCC AR5 and several previous studies using SRES-A1B or RCP4.5 scenarios. Using a downscaling system consisting of a global atmospheric model, HiRAM, and the GFDL hurricane model, under the RCP4.5 scenario the global number of TCs decreases (−16.4%), that of CAT45 TCs increases (+28.3%), and the ratio of CAT45 TCs to all TCs increases (+53%) (Knutson et al., 2015). Under the SRES-A1B scenario, MRI-AGCM3.2H and related models simulate a reduction in the global number of TCs (−20.7%), insignificant changes in the global number of CAT45 TCs (+0.7%), and an increase in the ratio of CAT45 TCs to all TCs (48%), as shown in Sugi et al. (2016). Reduction in the total number of TCs and intensification of both the maximum surface wind and the mean precipitation are widely supported results. However, future changes in the number of CAT45 TCs have large uncertainty, because they depend on both the intensification of maximum surface wind and the reduction in the total number of TCs.

In individual ocean basins, large future reductions in TC genesis frequency occur in WNP (−42%), SIO (−44%) and SPA (−40%), while the changes are insignificant in ENP (−4%). The number of CAT45 TCs generally decreases, but increases in ENP (+88%) and does not change significantly in NIO and NAT. In IPCC AR5 only the changes in WNP and NAT are plotted, with large uncertainty, as there are insufficient data available for a complete assessment. Increasing rates of LMI of both surface wind speed and mean precipitation do not strongly depend on ocean basin but are larger in ENP and smaller in SPA. We can see large interbasin difference in the changes in TC activity metrics. The changes in TC activity metrics in the present study satisfy the relationships discussed in Knutson et al. (2015), which show that on an interbasin scale, the TC activity metrics and relative SST warming have a significant positive correlation. For example, the number of CAT45 TCs significantly increases in ENP where SST warming is relatively large, while it significantly decreases in SPA where SST warming is relatively small (see Figure S1a). We also note that there is a large uncertainty in TC activity change in individual ocean basins especially in ENP and NAT (Figure 4). Uncertainty from future SST warming patterns is found to be the main source of uncertainty in TC activity change in each ocean basin (see Figure S4 and Table S1).

5. Concluding Remarks

Using the d4PDF data set that contains high-resolution and 5, 000 year scale ensemble current and future climate simulations by MRI-AGCM3.2H, we have presented potential future changes in TC activity,

including detailed probability information under the 4 K warming scenario. Conclusions of the present study are as follows:

1. Annual TC genesis frequency in the global ocean decreases by −33% in the future climate. We have noted that the probability distributions of TC genesis frequency parametrically estimated by small ensemble simulations have large estimation errors, compared with the nonparametric probability distributions directly estimated by large-ensemble simulations.

2. Geographical TC occurrence frequencies decrease generally but increase near Hawaii and west of Senegal. Statistically significant increases in the very intense (CAT45) TC occurrence frequencies occur in the south of Japan, west of Mexico, and south of Madagascar, despite a significant decrease in total TC occurrence frequencies.

3. In interannual variations in WNP and NAT, almost all ensemble members simulate observed anomalous years of TC genesis frequency, showing these anomalous years may be a response to SST variation and be realized in high probability.

4. Globally, the number of CAT45 TCs decreases by 13%, in contrast to the results in IPCC AR5 and previous studies using SRES-A1B or RCP4.5 scenarios. Lifetime maximum intensity (LMI) of surface wind speed of TC is enhanced by 9%, and that of mean precipitation rate near the TC center is amplified by 28%.

5. In individual ocean basins, TC genesis frequency significantly decreases in WNP (−42%), SIO (−44%), and SPA (−40%) and does not change significantly in ENP (−4%). Regional TC activity, relatively, increases in ENP and decreases in SPA, which depends on regional differences in SST warming as discussed in Knutson et al. (2015). The number of CAT45 TCs has larger uncertainties and interbasin difference than the other metrics and increases drastically in ENP (+88%).

In IPCC AR5, potential future changes in TC activity metrics at the end of the 21st century for the SRES-A1B-like scenario are estimated by expert judgment using recent studies (Christensen et al., 2013). The estimation is rather subjective and relies on limited numbers of samples. In contrast, we investigated potential future changes in the TC activity metrics under the RCP8.5 scenario in a more objective manner.

Large-ensemble simulations drastically reduce the uncertainty of future TC activity originating from atmospheric internal variations and show that future SST patterns generate large uncertainty in regional TC activity. In addition, uncertainty in TC activity changes arises from the use of different future climate scenarios, atmospheric models (e.g., Horn et al., 2014; Walsh et al., 2015), and TC detection methods. Further study is needed to attempt assessments of future change in TC activity by both coordinated model inter comparison and various TC detection methods.

However, the present study provides important information especially for assessing TC activity probabilistically even in extreme and regional cases, which may help policy making related to future climate change.

References

Bengtsson, L., Hodges, K. I., Esch, M., Keenlyside, N., Kornblueh, L., Luo, J. J., & Yamagata, T. (2007). How may tropical cyclones change in a warmer climate? *Tellus Series A: Dynamic Meteorology and Oceanography*, *59*(4), 539–561. https://doi.org/10.1111/j.1600-0870.2007.00251.x

Camargo, S. J. (2013). Global and regional aspects of tropical cyclone activity in the CMIP5 models. *Journal of Climate*, *26*(24), 9880–9902. https://doi.org/10.1175/JCLI-D-12-00549.1

Christensen, J. H., Krishna Kumar, K., Aldrian, E., An, S.-I., Cavalcanti, I. F. A., de Castro, M., … Zhou, T. (2013). *Climate Phenomena and their Relevance for Future Regional Climate Change, in Climate Change 2013: The Physical Science Basis. Contribution of Working Group I to the Fifth Assessment Report of the Intergovernmental Panel on Climate Change*. In T. F. Stocker et al. (Eds.) (chap. 14, pp. 1217–1308). New York, USA: Cambridge University Press.

Gualdi, S., Scoccimarro, E., & Navarra, A. (2008). Changes in tropical cyclone activity due to global warming: Results from a high-resolution coupled general circulation model. *Journal of Climate*, *21*(20), 5204–5228. https://doi.org/10.1175/2008JCLI1921.1

Hirahara, S., Ishii, M., & Fukuda, Y. (2014). Centennial-scale sea surface temperature analysis and its uncertainty. *Journal of Climate*, *27*(1), 57–75. https://doi.org/10.1175/JCLI-D-12-00837.1

Horn, M., Walsh, K., Zhao, M., Camargo, S. J., Scoccimarro, E., Murakami, H., … Oouchi, K. (2014). Tracking scheme dependence of simulated tropical cyclone response to idealized climate simulations. *Journal of Climate*, *27*(24), 9197–9213. https://doi.org/10.1175/JCLI-D-14-00200.1

Kawase, H., Murata, A., Mizuta, R., Sasaki, H., Nosaka, M., Ishii, M., & Takayabu, I. (2016). Enhancement of heavy daily snowfall in central Japan due to global warming as projected by large ensemble of regional climate simulations. *Climatic Change*, *139*(2), 265–278. https://doi.org/10.1007/s10584-016-1781-3

Knutson, T. R., McBride, J. L., Chan, J., Emanuel, K., Holland, G., Landsea, C., … Sugi, M. (2010). Tropical cyclones and climate change. *Nature Geoscience*, *3*(3), 157–163. https://doi.org/10.1038/ngeo779

Knutson, T. R., Sirutis, J. J., Zhao, M., Tuleya, R. E., Bender, M., Vecchi, G. A., … Chavas, D. (2015). Global projections of intense tropical cyclone activity for the late twenty-first century from dynamical downscaling of CMIP5/RCP4.5 scenarios. *Journal of Climate*. https://doi.org/10.1175/JCLI-D-15-0129.1

Lighthill, J., Holland, G., Gray, W. M., Landsea, C. W., Craig, G., Evans, J., … Guard, C. (1994). Global glimate change and tropical cyclones. *Bulletin of the American Meteorological Society*, *75*(11), 2147–2158.

Ma, J., & Xie, S. P. (2013). Regional patterns of sea surface temperature change: A source of uncertainty in future projections of precipitation and atmospheric circulation. *Journal of Climate*, *26*(8), 2482–2501. https://doi.org/10.1175/JCLI-D-12-00283.1

Manganello, J. V., Hodges, K. I., Dirmeyer, B., Kinter, J. L. III, Cash, B. A., Marx, L., … Wedi, N. (2014). Future changes in the western North Pacific tropical cyclone activity projected by a multidecadal simulation with a 16-km global atmospheric GCM. *Journal of Climate*, *27*(20), 7622–7646. https://doi.org/10.1175/JCLI-D-13-00678.1

McBride, J., Emanuel, K., Landsea, C., Holland, G., Willoughby, H., Chan, J., & Heming, J. (2006). Statement on tropical cyclones and climate change, WMO Int. Work. Trop. Cyclones, (November), 1–13.

Mizuta, R., Murata, A., Ishii, M., Shiogama, H., Hibino, K., Mori, N., … Kimoto, M. (2016). Over 5000 years of ensemble future climate simulations by 60 km global and 20 km regional atmospheric models. *Bulletin of the American Meteorological Society*. https://doi.org/10.1175/BAMS-D-16-0099.1

Mizuta, R., Yoshimura, H., Murakami, H., Matsueda, M., Endo, H., Ose, T., … Kitoh, A. (2012). Climate simulations using MRI-AGCM3.2 with 20-km Grid. *Journal of the Meteorological Society Japan*, *90A*, 233–258. https://doi.org/10.2151/jmsj.2012-A12

Murakami, H., Hsu, P.-C., Arakawa, O., & Li, T. (2014). Influence of model biases on projected future changes in tropical cyclone frequency of occurrence*. *Journal of Climate*, *27*(5), 2159–2181. https://doi.org/10.1175/JCLI-D-13-00436.1

Murakami, H., Mizuta, R., & Shindo, E. (2012). Future changes in tropical cyclone activity projected by multi-physics and multi-SST ensemble experiments using the 60-km-mesh MRI-AGCM. *Climate Dynamics*, *39*(9–10), 2569–2584. https://doi.org/10.1007/s00382-011-1223-x

Murakami, H., Vecchi, G. A., Underwood, S., Delworth, T. L., Wittenberg, A. T., Anderson, W. G., … Zeng, F. (2015). Simulation and prediction of category 4 and 5 hurricanes in the high-resolution GFDL HiFLOR coupled climate model. *Journal of Climate*, *28*(23), 9058–9079. https://doi.org/10.1175/JCLI-D-15-0216.1

Murakami, H., Wang, B., Li, T., & Kitoh, A. (2013). Projected increase in tropical cyclones near Hawaii. *Nature Climate Change*, *3*(8), 749–754. https://doi.org/10.1038/nclimate1890

Murakami, H., Wang, Y., Yoshimura, H., Mizuta, R., Sugi, M., Shindo, E., … Kitoh, A. (2012). Future changes in tropical cyclone activity projected by the new high-resolution MRI-AGCM. *Journal of Climate*, *25*(9), 3237–3260. https://doi.org/10.1175/JCLI-D-11-00415.1

Ogata, T., Mizuta, R., Adachi, Y., Murakami, H., & Ose, T. (2015). Effect of air-sea coupling on the frequency distribution of intense tropical cyclones over the northwestern Pacific. *Geophysical Research Letters*, *42*, 10,415–10,421. https://doi.org/10.1002/2015GL066774

Roberts, M. J., Vidale, P. L., Mizielinski, M. S., Demory, M. E., Schiemann, R., Strachan, J., … Camp, J. (2015). Tropical cyclones in the UPSCALE ensemble of high-resolution global climate models. *Journal of Climate*, *28*(2), 574–596. https://doi.org/10.1175/JCLI-D-14-00131.1

Strachan, J., Vidale, P. L., Hodges, K., Roberts, M., & Demory, M. E. (2013). Investigating global tropical cyclone activity with a hierarchy of AGCMs: The role of model resolution. *Journal of Climate*, *26*(1), 133–152. https://doi.org/10.1175/JCLI-D-12-00012.1

Sugi, M., Murakami, H., & Yoshida, K. (2016). Projection of future changes in the frequency of intense tropical cyclones. *Climate Dynamics*, *49*, 619–632. https://doi.org/10.1007/s00382-016-3361-7

Sugi, M., Murakami, H., & Yoshimura, J. (2009). A reduction in global tropical cyclone frequency due to global warming. *Solaiat*, *5*, 164–167. https://doi.org/10.2151/sola.2009-042

Taylor, K. E., Stouffer, R. J., & Meehl, G. A. (2012). An Overview of CMIP5 and the Experiment Design. *Bulletin of the American Meteorological Society*, *93*, 485–498. https://doi.org/10.1175/BAMS-D-11-00094.1

Unisys (2015). Unisys weather hurricane tropical data. [Available at http://weather.unisys.com/hurricane/.]

Walsh, K. J. E., Camargo, S. J., Vecchi, G. A., Daloz, A. S., Elsner, J., Emanuel, K., … Henderson, N. (2015). Hurricanes and climate: The U.S. CLIVAR working group on hurricanes. *Bulletin of the American Meteorological Society*, *96*(6), 997–1017. https://doi.org/10.1175/BAMS-D-13-00242.1

Wehner, M. P., Reed, K. A., Stone, D., Collins, W. D., & Bacmeister, J. (2015). Resolution dependence of future tropical cyclone projections of CAM5.1 in the US CLIVAR Hurricane Working Group idealized configurations. *Journal of Climate*, *28*, 3905–3925. https://doi.org/10.1175/JCLI-D-14-00311.1